

PACS 85.30.Kk

Impact of traps on current-voltage characteristic of $n^+ - n - n^+$ diode

P.M. Kruglenko

*V. Lashkaryov Institute of Semiconductor Physics, NAS of Ukraine,
41, prospect Nauky, 03680 Kyiv, Ukraine,
E-mail: p.kruglenko@gmail.com*

Abstract. A model of $n^+ - n - n^+$ diode is analyzed using analytical and numerical methods. First, it was conducted a phase-plane analysis, which was aimed at further calculations for low and high injection approximations. A numerical method was used to calculate changes of the field, bias and concentration throughout the diode for different current values. Expected depletion of free-charge carriers near the anode, and enrichment near the cathode was observed. Current-voltage characteristics were built for different concentrations of traps in base. Increasing bias for same value of current with increasing traps concentration was predicted.

Keywords: semiconductor diode, phase-plane, trap influence.

Manuscript received 02.02.17; revised version received 13.04.17; accepted for publication 14.06.17; published online 18.07.17.

1. Introduction

Semiconductors with defects were a subject of intense researches as early as 1940s [1]. Later development of semiconductor physics and technology allowed creating the close to perfect defect-free materials and devices, including diodes [2]. However, with increasing ability to make nano-sized diodes, processes at surfaces of interfaces became more influential. The presence of traps in semiconductors contributes to different physical phenomena. Unlike defect-free semiconductors, which have quadratic current-bias characteristic [3], diodes with defects exhibit slow rise of current until critical voltage is reached, and power-law rise after critical voltage [4]. The presence of dopants in regions with traps also has a large effect on currents in semiconductor devices [5]. Dopants together with the Frenkel effect also control shape of the current-voltage characteristics [6]. Another effect that is introduced by traps in semiconductor devices are noise sources caused by random trapping and detrapping of charge carriers (see [7] for bulklike samples and [8] for nanowires/nanoribbons). The surface noise can be considerably suppressed due to Coulomb correlations between trapped and conducting electrons [9].

In this work, we calculate the current-bias characteristics alongside distributions of the field, potential and concentrations of free and trapped carriers in the short diode with dopants and traps. We employ the phase-plane method [10] that allows to make qualitative conclusions on transport in the short diode. We include in the model a finite-length base and infinite contacts with higher doping concentration. Numerical calculations were performed using the numerical methods in general case, but analytical approximations were also used for low and high injection modes.

2. Steady-state transport model and main equations

The Poisson equation describes the field change in the base

$$\frac{dE}{dx} = -\frac{e_0}{\epsilon\epsilon_0}(n + N - N_b) \quad (1)$$

and in contact

$$\frac{dE}{dx} = -\frac{e_0}{\epsilon\epsilon_0}(n - N_c), \quad (2)$$

where E is the field, n, N are electron density of free charges and charges captured by traps, N_b, N_c – dopant concentrations in the base and contacts, x is the coordinate, e_0 – positive electron charge, ϵ, ϵ_0 are the relative and vacuum permeabilities.

For the density change, we consider continuity equations for base with generation and recombination of free particles

$$\frac{\partial n}{\partial t} + \text{div } \vec{i} = G - R, \quad (3)$$

$$\frac{\partial N}{\partial t} = -G + R. \quad (4)$$

In the case of contact, generation and recombination terms are absent:

$$\frac{\partial n}{\partial t} + \text{div } \vec{i} = 0, \quad (5)$$

where $\vec{i} = -\frac{\vec{j}}{e_0}$ is the charge flow equal to current density divided by electron charge, $G = \gamma^+ N$, $R = \gamma^- n(N_t - N)$ are the generation and recombination terms, N_t is the density of traps, γ^+, γ^- are coefficients.

For the stationary problem, the time derivatives disappear, and we obtain the Poisson equations (1), (2) and constant current density that can be defined using the drift-diffusion equation

$$\frac{j}{e_0} = D \frac{dn}{dx} + \mu n E, \quad (6)$$

where D is the diffusion coefficient, μ – mobility.

Diffusion can be expressed through mobility $D = \frac{kT}{e_0} \mu$, where k is the Boltzmann constant, T – temperature. The density of trapped charges we can get from (4)

$$N = \frac{n}{\frac{\gamma^+}{\gamma^-} + n} N_t. \quad (7)$$

Dimensionless equations look like

$$\frac{dE}{dx} = -n - \frac{n}{\kappa + n} N_t + N_b \quad (8)$$

for field in the base,

$$\frac{dE}{dx} = -n + N_c \quad (9)$$

for field in the contacts and

$$\frac{dn}{dx} = j - nE \quad (10)$$

for the drift-diffusion equation (6) throughout the diode.

The parameter $\kappa = \frac{\gamma^+}{\gamma^- N_{ch}}$ describes relation between generation and recombination processes. Characteristic

parameters are N_{ch} for concentration, $l_D = \sqrt{\frac{\epsilon \epsilon_0 kT}{N_{ch} e_0^2}}$ –

Debye length for the set concentration, $E_D = \frac{kT}{el_D}$ –

Debye field, $j_{ch} = \frac{kT \mu N_{ch}}{l_D}$ – for current density.

3. General case: the phase-plane analysis

We transform dimensionless equations (8), (10) into the field-concentration differential equation

$$\frac{dE}{dn} = \frac{-n^2 - n(N_t + \kappa - N_b) + \kappa N_b}{(j - nE)(\kappa + n)} \quad (11)$$

which we can analyze using calculated separatrix guidelines:

$$E = \frac{j}{N_{crt}} + (n - N_{crt}) \frac{-j \pm \sqrt{j^2 + \frac{4N_{crt}^3 \sqrt{(N_b - N_t - \kappa)^2 + 4N_b k}}{\kappa + N_{crt}}}}{2N_{crt}^2} \quad (12)$$

and such properties as: the null derivative on $n = N_{crt}$ line, infinity derivative at $E = \frac{j}{n}$ curve, derivative equal

to $\frac{N_b}{j}$ at $n = 0$. N_{crt} here is the critical concentration for Eq. (10) equal to

$$N_{crt} = \frac{N_b - N_t - \kappa + \sqrt{(N_b - N_t - \kappa)^2 + 4N_b \kappa}}{2}. \quad (13)$$

Similar and simpler equations (no traps, hence terms with N_t and κ disappear) can be written for

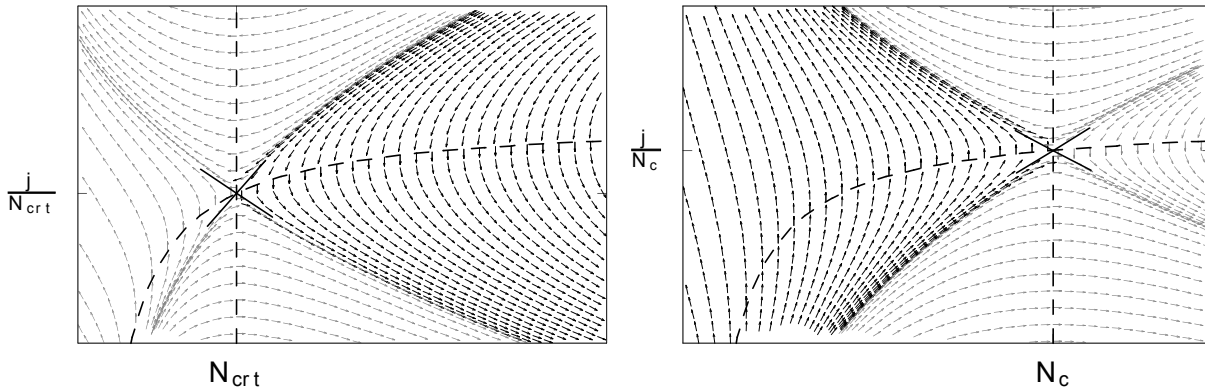


Fig. 1. Phase planes. Solid lines represent separatrix guidelines, dashed – characteristic lines. Four regions where the phase plane is divided by the separatrix define different behaviour of Eq. (11).

equations describing movement of the charged particle in the contact.

Examples of phase planes are shown in Figs 1, 2 and 3. All of them show relation of field (vertical axis) and concentration (horizontal axis). Phase planes shown in Fig. 1 describe all possible field and concentration relations in the base and contact of semiconductor, with all possible boundary conditions. For instance, darker trajectories in the phase plane with the critical point N_{crit} correspond to any concentration-field relations inside base (trajectories have lower concentration inside the base, and higher concentration at interfaces; and field is constantly decreased). Likewise, darker trajectories in the phase plane with the critical point N_c correspond to relations in the contact (maximum of the concentration for particular trajectory can be taken as starting and ending points, with the concentration decreasing in cathode, and rising in anode; and field growing in both contacts). It should be noted that different intersections of darker trajectories from those phase planes depict all solutions to equations (8)-(10) in conditions of equal stronger doped contacts and weaker doped base. When moving along the particular line on the phase plane, one can determine the distance between two points by integrating the equation (10), for example. Movement from or to critical point $N_{crit}, \frac{j}{N_{crit}}$ (along any of the separatrix) gives infinite distance, which can be used to model infinitely large contacts, as in our case.

Fig. 2 shows few integral paths for the base and separatrix for the contact. A solution to the system of equations (8)-(10) should start in the critical point for contact $\left(N_c, \frac{j}{N_c}\right)$, then moving along separatrix one reaches the field maximum at the left interface, then moving along the path integral for the base to the right interface and then again one reaches the critical point in the contact by using different separatrix.

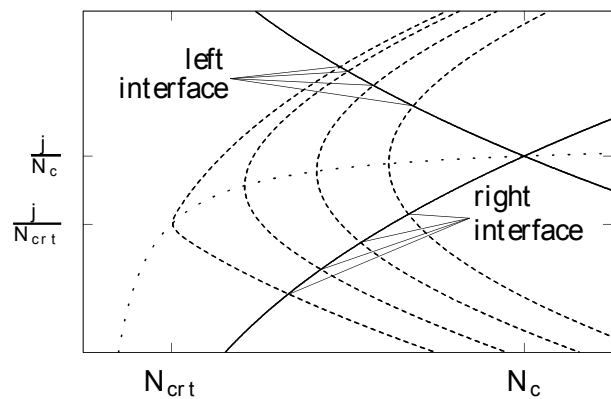


Fig. 2. Solutions for both the contact and base are shown on the same phase plane. Solid line shows separatrices for the contact, dashed – integral paths for different intercontact distances; both critical points for the base and contact lie on the dotted line $\frac{j}{n}$. The top intersection point of separatrix and integral path represent the left interface of diode, bottom – right interface.

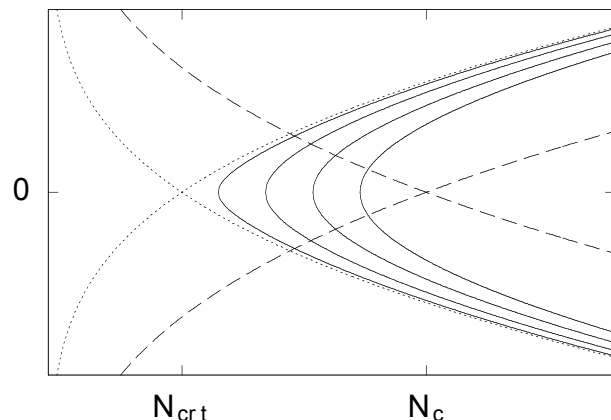


Fig. 3. Phase plane for diode without injection. Dotted line is the separatrix for the base, dashed – for the contact, and solid lines represent solutions for the base. Unlike previous Figs 1 and 2, these lines can be built analytically.

4. Equilibrium distributions in the unbiased diode

In the absence of current, equations (8)-(10) can be solved analytically. The field-concentration dependence can be written as

$$E_0 = \pm \sqrt{2 \left(n_0 - N_{\min} + N_t \log \frac{\kappa + n_0}{\kappa + N_{\min}} - N_b \log \frac{n_0}{N_{\min}} \right)}, \quad (14)$$

$$E_0 = \pm \sqrt{2 \left(n_0 - N_c \left(1 + \log \frac{n_0}{N_c} \right) \right)} \quad (15)$$

for the base and contact, respectively. N_{\min} defines the minimum concentration in the base.

A dependence of the concentration on the coordinate can be found from the integral expression

$$x = - \int \frac{n}{n_0 E_0(n_0)} dn. \quad (16)$$

The equations give the expected result (Fig. 3): symmetrical distribution of charged particles concentration and the potential in diode, as well as the asymmetrical field distribution.

5. Regime of low injection

We consider a low current in the diode. In this case, we can expect a solution in the form $E = E_0 + E_1 + \frac{j}{N^*}$, $n = n_0 = n_1$, where E_0, n_0 denote unbiased solutions, $E_1 + \frac{j}{N^*}, n_1$ – corrections for low injection. N^* is the dopant concentration N_c in the case of contact and the minimum concentration N_{\min} in the case of base. Correction for the field is split by two terms for convenience – it requires E_1 term to be equal to zero in the N^* point.

Solving the equations (8)-(10) simplified to the first order in respect to E_1, n_1 and current density j , we get

$$E_1 = -j E_0' \int_0^x \frac{E_0''}{E_0'^2 E_0} \int_0^{x'} E_0' \left(\frac{1}{n_0} - \frac{1}{N^*} \right) dx'' dx', \quad (17)$$

$$n_1 = -n_0 E_0 \frac{E_1}{E_0'} + j \frac{n_0}{E_0'} \int_0^x E_0' \left(\frac{1}{n_0} - \frac{1}{N^*} \right) dx', \quad (18)$$

where

$$E_0' = -n_0 - \frac{n_0 N_t}{\kappa + n_0} + N_b, \quad (19)$$

$$E_0'' = n_0 E_0 \left(1 + \frac{\kappa N_t}{(\kappa + n_0)^2} \right) \quad (20)$$

for the base, and

$$E_0' = -n_0 + N_c, \quad (21)$$

$$E_0'' = n_0 E_0 \quad (22)$$

for the contact.

6. Regime of high injection under virtual cathode approximation

Under the high current, we can neglect the diffusion term $\frac{dn}{dx}$ in (10), and equations become solvable in respect to coordinate x

$$x = \frac{E}{N_b} + \frac{j}{\kappa N_b^2 (N_{crt} - N_2)} \times \left((\kappa N_b - \kappa N_2 - N_t N_2) \log \left(1 + \frac{E}{j} \frac{\kappa N_b}{N_2} \right) - (\kappa N_b - \kappa N_{crt} - N_t N_{crt}) \log \left(1 + \frac{E}{j} \frac{\kappa N_b}{N_{crt}} \right) \right) \quad (23)$$

for the base and

$$x = \frac{E}{N_c} + \frac{j}{N_c^2} \log \left(1 - \frac{E}{j} N_c \right) \quad (24)$$

$$x = x_c + \frac{E - E_c}{N_c} + \frac{j}{N_c^2} \log \left(1 + \frac{E - E_c}{E_c - \frac{j}{N_c}} \right) \quad (25)$$

for the cathode and anode, respectively. N_c denotes another critical point for the equation (11) with the negative value, E_c, x_c are the field and coordinate at the interface between the base and anode.

Since Eq. (10) without diffusion gives the simple field-concentration dependence $E = -\frac{j}{n}$, all the integral

paths lay on the same line in the phase plane. Because of it, we can't use intersections of integral paths corresponding to the base and contact to determine the values of field and concentration at the interface. Hence, we should use virtual cathode approximation that puts the field maximum $\frac{dU}{dx} = 0$ for $x = 0$ at the interface between the cathode and base. This approximation requires

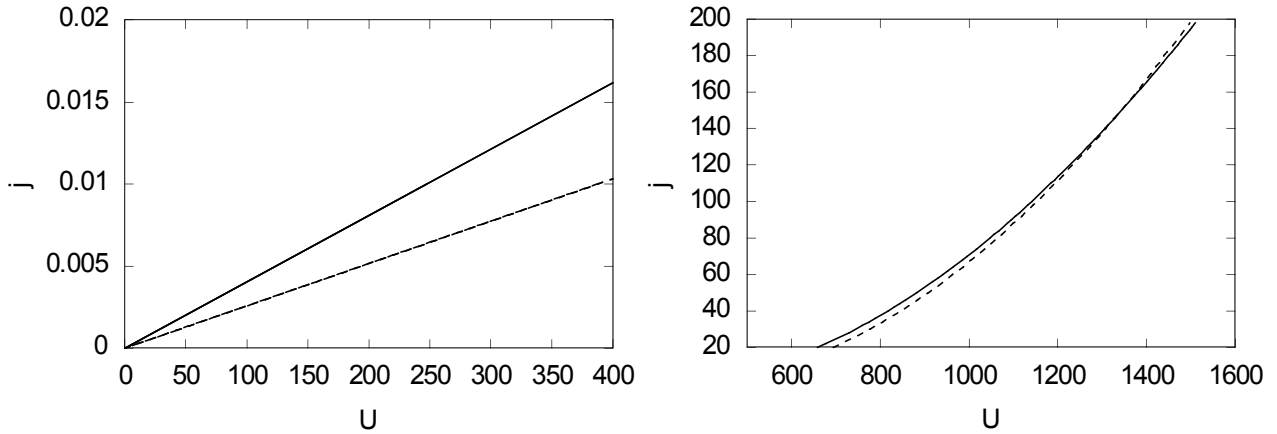


Fig. 4. Comparison of approximation and numerical calculation. Solid line denotes the numerical result, dashed line – approximation for small injection and high injection, respectively.

the current density to be greater than not only diffusion term, but also doping concentration of the contact N_c .

See Fig. 4 for comparison between numerical results and approximations for high and low injection.

7. General case of arbitrary injection. Numerical results

To solve equations (8)-(10) in general case, we will use the Runge–Kutta method. Plotting the integral paths for the base and contact, then we intersect them to determine interface values of field and concentration along with base width. By manipulating the minimal concentration in the base N_{\min} , we can change the width of base, and get it to the predefined value. After calculating basic relations for the field, concentrations of free and trapped charged particles, we can calculate and plot the potential of the diode at various current densities.

As a result, we get the expected shift of the concentration plot in direction to the anode with increasing injection, as seen in the inlet of Fig. 5.

The above analysis was done in dimensionless variables. To apply these results to particular diodes, we present the normalization parameters in the table below. Values for InAs at 77 K are not included, since the calculated mean free path (L_{fp}) was comparable to intercontact distance, which does not satisfy our model. All the values are in SI units, except L_{fp} , which is dimensionless. Values for mobility and other characteristics of materials were taken from different articles [11-14] and books [15, 16].

Fig. 6 depicts the dependence current-voltage on the trap concentration in the base. A higher potential for the same level of injection can be required with increasing the concentration of traps. This shift to higher voltages can be explained by trapped injected carriers that generate push-back voltage until all the traps are filled, at which point the current sharply rises [6]. Our model doesn't accommodate for breakdown field, but if we take Si as example, its breakdown voltage would lie near 240 V, and Fig. 6 goes only to 12 V.

	T, K	$N_{ch}, \frac{1}{m^3}$	L_{fp}	L_d, m	$E_d, \frac{V}{m}$	$j_{ch}, \frac{A}{m^2}$	U_{ch}, V
Si	300	10^{20}	0.2	$4.1 \cdot 10^{-07}$	$6 \cdot 10^4$	10^5	0.03
Si	77	10^{20}	1.7	$2.1 \cdot 10^{-07}$	$3 \cdot 10^4$	$6 \cdot 10^5$	0.007
Ge	300	10^{20}	0.4	$4.8 \cdot 10^{-07}$	$5 \cdot 10^4$	$3 \cdot 10^5$	0.03
Ge	77	10^{20}	2.8	$2.4 \cdot 10^{-07}$	$3 \cdot 10^4$	10^6	0.007
InAs	300	10^{22}	4.9	$4.7 \cdot 10^{-08}$	$6 \cdot 10^5$	$2 \cdot 10^9$	0.03
GaAs	300	10^{21}	1.1	$1.4 \cdot 10^{-07}$	$2 \cdot 10^5$	$2 \cdot 10^7$	0.03
GaAs	77	10^{21}	2.0	$6.9 \cdot 10^{-08}$	$1 \cdot 10^5$	$3 \cdot 10^7$	0.007
GaN	300	10^{20}	3.2	$3.6 \cdot 10^{-07}$	$7 \cdot 10^4$	$5 \cdot 10^6$	0.03
GaN	77	10^{20}	0.8	$1.8 \cdot 10^{-07}$	$4 \cdot 10^4$	$6 \cdot 10^5$	0.007

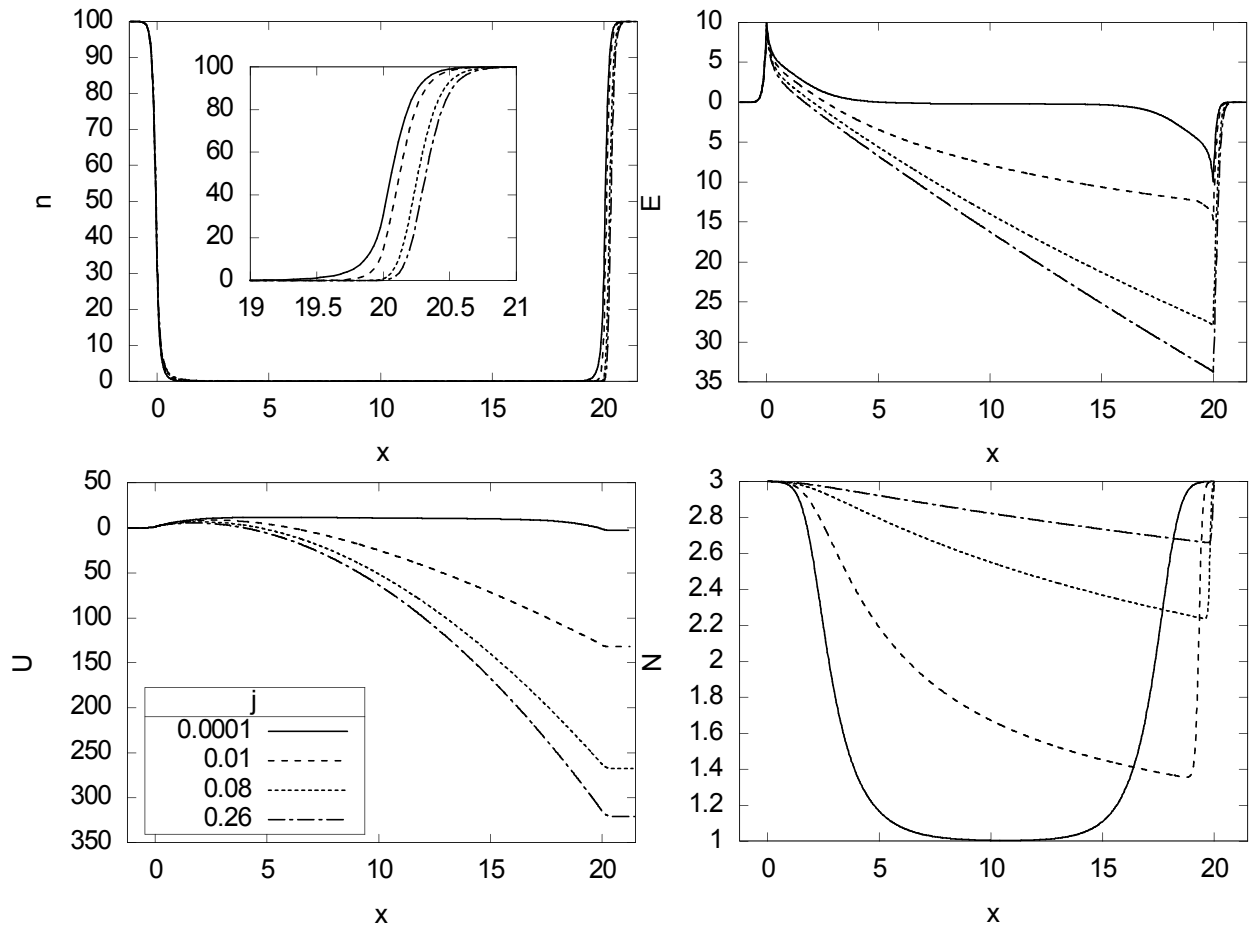


Fig. 5. Concentrations of free (n) and trapped (N) particles, field (E) and potential (U) through diode, for different current density. Legend for current density on potential graph applies to all others as well. Left and right interfaces located at the coordinate values 0 and 20, respectively. Inside free particles graph, the inset scales up the version of right interface. For example, for particular case of Si, at room temperature, width of the base would be $8 \cdot 10^{-6}$ m, current density would be scaled from 10 to $26 \cdot 10^3 \frac{A}{m^2}$, and maximum potential drop would be 9 V.

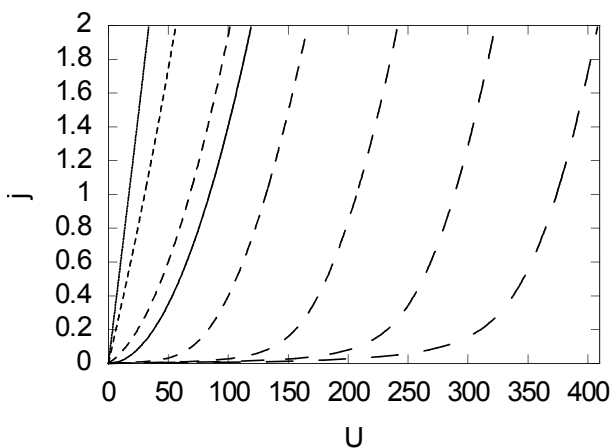


Fig. 6. Current-voltage characteristics. Solid line calculated according to Gurney–Mott law, dashed – numerical results for different concentrations of trapped charges. $N_t = 0, 0.5, 1, 1.5, 2, 2.5, 3$ from shorter dashed lines to the longer ones, respectively.

8. Conclusion

The introduced model is viable for both analytical and numerical analysis. The phase-plane analysis gives general prediction of numerical results for concentration and field change inside the diode. From these results, we can see the dependence of current-bias characteristic from traps concentration in the base, with a linear characteristic corresponding to the concentration of traps being smaller than the dopant one, and a power like characteristic for traps concentrations higher than that of dopant, which shifts further to higher voltages with increasing the traps concentration, due to push-back voltage generated by trapped injected carriers.

References

1. Pekar S.I. Theory of the contact between metal and dielectric or semiconductor. *Zhurnal Eksperiment.*

- and *Teoreticheskoi Fiziki*. 1940. **10**. P. 341–348 (in Russian).
- Weaver J.H. *Formation of Defect-Free Metal/Semiconductor Contacts*. Minnesota University, Minneapolis Department of Chemical Engineering and Materials Science, 1992.
 - Mott N.F. and Gurney R.W. *Electronic Processes in Ionic Crystals*. Clarendon Press, 1940.
 - Smith R.W. and R.A. Space-charge-limited currents in single crystals of cadmium sulfide. *Phys. Rev.* 1955. **97**, No. 6. P. 1531–1537.
 - Zhang Yuan and Blom P.W.M. Field-assisted ionization of molecular doping in conjugated polymer. *Organic Electronics*. 2010. **11**. P. 1261–1267.
 - Zhang X.-G. and Pantelides S.T. Theory of space charge limited currents. *Phys. Rev. Lett.* 2012. **108**, No. 26. P. 266602.
 - Kogan S. *Electronic Noise and Fluctuations in Solids*. Cambridge University Press, 2008.
 - Sydoruk V.A., Vitusevich S.A., Hardtdegen H. et al. Electric current and noise in long GaN nanowires in the space-charge limited transport regime. *Fluctuation and Noise Lett.* 2017. **16**, No. 1. P. 1750010 (12 p.).
 - Kochelap V.A., Sokolov V.N., Bulashenko O.M., and Rubi J.M. Coulomb suppression of surface noise. *Appl. Phys. Lett.* 2001. **78**, No. 14. P. 2003–2005.
 - Sokolov V.N. et al. Phase-plane analysis and classification of transient regimes for high-field electron transport in nitride semiconductors. *J. Appl. Phys.* 2004. **96**. P. 6492–6503.
 - Li Sheng S. and Thurber W.R. The dopant density and temperature dependence of electron mobility and resistivity in *n*-type silicon. *Solid-State Electron.* 1977. **20**. P. 609–616.
 - Fistul V.I., Iglitsyn M.I. and Omelyanovskii E.M. Mobility of electrons in germanium strongly doped with arsenic. *Fizika tverdogo tela*. 1962. **4**, No. 4. P. 784–785 (in Russian).
 - Andrianov D.G. et al. Interaction of carriers with localized magnetic moments in InSb-Mn and InAs-Mn. *Fizikai tekhnika poluprovodnikov*. 1977. **11**, No. 7. P. 738–742 (in Russian).
 - Chin V.W.L., Tansley T.L. and Osotchan T. Electron mobilities in gallium, indium, and aluminum nitrides. *J. Appl. Phys.* 1994. **75**. P. 7365–7372.
 - Sze S.M. and Ng Kwok K. *Physics of Semiconductor Devices*. John Wiley & Sons, 2006.
 - Rode D.L. Ch. 1: Low-Field Electron Transport. *Semiconductors and Semimetals*. 1975. **10**. P. 1–89.